A THESIS FOR THE DEGREE OF MASTER OF SCIENCE

Lipase-catalyzed synthesis of erythorbyl myristate as a novel multi-functional food emulsifier with antioxidative and antibacterial properties

항산화 및 항균능을 가지는 신규 다기능성
식품 유화제 에리소르빌 미리스테이트의
라이페이스 기반 효소적 합성

August, 2020

Department of Agricultural Biotechnology

Seoul National University

Jaeho Myeong

석사학위논문

Lipase-catalyzed synthesis of erythorbyl myristate as a novel multi-functional food emulsifier with antioxidative and antibacterial properties

지도교수 장 판 식

이 논문을 석사학위 논문으로 제출함

2020년 8월

서울대학교 대학원

농 생 명 공 학 부

명 재 호

명재호의 석사 학위논문을 인준함

2020년 8월

위원장 최 영 진 (인)

부위원장 장 판 식 (인)

위원 강 동 현 (인)

Abstract

Erythorbyl myristate, a promising multi-functional emulsifier with antioxidative and antibacterial properties, was synthesized by enzymatic esterification of erythorbic acid and myristic acid using immobilized lipase (Novozym 435®). Liquid chromatography–electrospray ionization–mass spectrometry and two-dimensional correlation spectrometry, as well as proton nuclear magnetic resonance analyses, identified the structure of the product as 6-*O*-myristoyl-erythorbic acid. The multi-functionality of erythorbyl myristate was evaluated in terms of its emulsification, antioxidative, and antibacterial properties. The hydrophilic–lipophilic balance (11.5) and *n*-octanol/water partition coefficient (5.02) were calculated from erythorbyl myristate molecular structure and critical micelle concentration (0.33 mM) was measured using isothermal titration calorimetry; the results indicated that erythorbyl myristate could form an oil-in-water emulsion with high hydrophobicity. Next, the radical scavenging activity of erythorbyl myristate1 was determined using 2,2'-azino-bis(3-ethylbenzothiazoline-6-sulfonic acid)

(ABTS) and 2,2-diphenyl-1-picryl-hydrazyl-hydrate (DPPH) assays. The radical scavenging activity of erythorbyl myristate, which is derived from erythorbic acid, had a half-maximal effective concentration of 34.43±1.54 and 35.77±0.04 μM according to the ABTS and DPPH assays, respectively. Finally, antibacterial property screening demonstrated that erythorbyl myristate exerted both bacteriostatic and bactericidal activities on Gram-positive foodborne pathogens such as *Staphylococcus aureus* (minimum inhibitory concentration: 0.50–0.60 mM; minimum bactericidal concentration: 0.60–1.00 mM) and *Bacillus cereus* (minimum inhibitory concentration: 0.025–0.10 mM; minimum bactericidal concentration: 0.05–0.10 mM). However, erythorbyl myristate was ineffective against Gram-negative foodborne pathogens such as *Escherichia coli* and *Salmonella* Typhimurium. Transmission electron microscopy analysis suggested that alteration of membrane permeability was the mechanism for the antibacterial property of erythorbyl myristate. Therefore, erythorbyl myristate has potential as an excellent multi-functional emulsifier with antioxidative and antibacterial properties for use in the food industry.

Keywords: Erythorbyl myristate, lipase-catalyzed esterification, multi-functional emulsifier, emulsifying property, antioxidative property, antibacterial property

Student number: 2018-23305

Contents

List of tables

List of figures

(LC–ESI–MS) and protein nuclear magnetic resonance (^{1}H-NMR) analyses of the product from lipase-catalyzed synthesis of erythorbyl myristate. (a) LC chromatogram of purified erythorbyl myristate obtained using an ultraviolet detector. (b) Mass spectrum of the peak at 2.9 min retention time in the LC chromatogram. (c) Two-dimensional correlation spectrometry ^{1}H-NMR spectrum of purified erythorbyl myristate. A: tetramethylsilane; B: dimethyl sulfoxide-d_6; C: H_2O; D: D_2O.

Fig. 4. Molecular diagrams of erythorbyl myristate structure used to calculate emulsifying properties including (a) the hydrophilic–lipophilic balance based on the Davies method and (b) the *n*-octanol/water partition coefficient (log *P*) based on the atom/fragment contribution method.

Fig. 5. Calorimetric titration thermogram of 20 mM erythorbyl myristate in 50% ethanol at 25°C. EM: erythorbyl myristate.

Fig. 6. Antioxidative property of erythorbyl myristate based on radical scavenging activity. (a) 2,2'-azino-bis (3-ethylbenzothiazoline-6-sulfonic acid) (ABTS) and (b) 2,2-diphenyl-1-picryl-hydrazyl-hydrate (DPPH) radical scavenging activity of erythorbyl myristate. EM: erythorbyl myristate.

Fig. 7. Bacteriostatic and bactericidal activities of erythorbyl myristate against Gram-positive pathogens. Growth curves of (a) *Staphylococcus aureus* ATCC 12692 and (b) *S. aureus* ATCC 29213 treated with 0.05–0.60 mM erythorbyl myristate. Growth curves of (c) *Bacillus cereus* ATCC 13061 and (d) *B. cereus* ATCC 10876 treated with 0.025–0.50 mM erythorbyl myristate. Viable cell counts of (e) *S. aureus* ATCC 12692 and (f) *S. aureus* ATCC 29213 treated with 0.01–1.00 mM erythorbyl myristate. Viable cell counts of (g) *B. cereus* ATCC 13061 and (h) *B. cereus* ATCC 10876 treated with 0.05–0.80 mM erythorbyl myristate. EM: erythorbyl myristate.

Fig. 8. Bacteriostatic and bactericidal activities of erythorbyl myristate against Gram-negative pathogens. Growth curves of (a) *Escherichia coli* ATCC 35150 and (b) *Salmonella* Typhimurium ATCC 43971 treated with 0.05–0.60

mM erythorbyl myristate. Viable cell counts of (c) *E. coli* ATCC 35150 and *S.* Typhimurium ATCC 43971 treated with 0.01–1.0 mM erythorbyl myristate. EM: erythorbyl myristate.

Fig. 9. Transmission electron micrograph of *Staphylococcus aureus* ATCC 12692 treated with the minimum inhibitory concentration (MIC) and 2×MIC of erythorbyl myristate.

Fig. 10. The putative mode of action of erythorbyl myristate targeting the cytoplasmic membrane of Gram-positive pathogens.

1. Introduction

An emulsion is defined as two immiscible liquids wherein droplets of one phase (the dispersed phase) are encapsulated within sheets of another phase (the continuous phase) (Chen & Tao, 2005). Among various emulsion systems, oil-in-water (O/W) emulsions, which consist of small lipid droplets dispersed in an aqueous medium (*e.g.*, milk, cream, beverage, dressing, sauce, and mayonnaise), have been used in the food, cosmetic, and pharmaceutical industries (Yang, Jiang, He, & Xia, 2012; Zhang, Zhang, Fang, & Liu, 2017). In emulsion-based products, especially emulsion-based foods, lipid oxidation and microbial contamination are considered major hazards (Luther et al., 2007). Lipids in emulsion are susceptible to oxidation in the presence of catalysts such as light or heat, leading to complex processes such as autoxidation, photooxidation, and thermal oxidation (Shahidi & Zhong, 2010). Free radicals are key factors that stimulate lipid oxidation in a process called rancidification (Frankel, 1984), which decreases the nutritional value and shelf life of emulsion-based foods. Another major hazard in emulsion-based foods, contamination by foodborne pathogens, can lead to outbreaks of foodborne illnesses such as diarrhea, vomiting, and fever (Maijala et al., 2001). Therefore, these hazards must be controlled by

appropriate strategies to enhance the quality and safety of emulsion-based foods.

Multi-functional emulsifiers represent a strategy for the prevention of these hazards. Precious studies synthesized erythorbyl laurate, the esterified product of the antioxidant erythorbic acid (hydrophilic moiety) and antibacterial lauric acid (lipophilic moiety), using immobilized lipase (Park, Lee, Sung, Lee, & Chang, 2011). The multi-functionality of erythorbyl laurate was evaluated in terms of its antioxidative, antibacterial, and emulsifying properties (Park, Jo, et al., 2018; Park, Lee, Jo, Choi, Lee, & Chang, 2017). Each emulsifier has different optimal conditions for emulsifications (Yuan, Gao, Mao, & Zhao, 2008). For example, commercial Tween emulsifiers (*e.g.*, Tween 20, Tween 40, Tween 60, and Tween 80) have different emulsifying properties based on their hydrophobic moieties (*i.e.*, fatty acid) despite having the same hydrophilic moiety. Therefore, the synthesis of various erythorbyl fatty acid esters is necessary for the manufacture of suitable multi-functional emulsifiers for use under specific emulsification conditions.

The objectives of this study were to synthesize a novel erythorbyl fatty acid ester by altering the hydrophobic moiety and evaluate its multi-functionality in terms of its emulsifying, antioxidative, and antibacterial

properties. Myristic acid was selected as the hydrophobic moiety for its antibacterial property (Kabara, Swieczkowski, Conley, & Truant, 1972). The emulsifying property of novel erythorbyl fatty acid ester were evaluated in terms of its hydrophilic–lipophilic balance (HLB) and *n*-octanol/water partition coefficient (log *P*). Its antioxidative property was evaluated in terms of radical scavenging activity, and its antibacterial property was evaluated using a broth micro-dilution test, viable cell count, and transmission electron microscopy (TEM) analysis.

2. Materials and methods

2.1. Materials

Immobilized lipase Novozym 435® (from *Candida antarctica* lipase immobilized onto macroporous acrylic resin) with a catalytic activity of 10,000 propyl laurate units/g was purchased from Novozymes (Bagsvaerd, Denmark). Erythorbic acid (≥ 98.0%) and myristic acid were purchased from Acros Organics (Geel, Belgium) and Daejung Chemicals & Metals Co. (Siheung, Republic of Korea), respectively. 1,1-Diphenyl-2-picrylhydrazyl (DPPH) and 2,2′-azino-bis-3-ethylbenzo-thiazoline-6-sulfonic acid (ABTS) were purchased from Sigma-Aldrich Co. (St. Louis, MO, USA). High-performance liquid chromatography (HPLC)-grade methanol, water, and acetic acid (J.T. Baker Co., Phillipsburg, NJ, USA) were filtered through a membrane filter (0.45 μm) before use. All other reagents were of analytical grade.

2.2. Lipase-catalyzed esterification

Esterification of erythorbic acid and myristic acid was conducted in a gas–solid–liquid multiphase system (GSL-MPS) (Fig. 1). Briefly, nitrogen gas was distributed through the glass filter (0.5 cm thickness, 27.5 μm pore size)

at a flow rate of 6.0 mL/min to a 10.0×12.0 cm 500 mL reaction vessel during the reaction. The reaction temperature was controlled by a water circulator to maintain a temperature of 70°C. Myristic acid (1.70 mol) was added into the reaction vessel and melted for 30 min for use as a liquid phase, followed by the addition of 0.85 mol erythorbic acid. The reaction was initiated by adding 0.12 g/mL Novozym 435® to the reaction vessel. After the reaction had finished, the reactant was filtrated through a glass filter by replacing the gas generator with a vacuum pump.

2.3. Product analysis using HPLC-UV/RI

The reactants were sampled at 12 h intervals and analyzed by HPLC. The reactants (20 μL) were dissolved in 980 μL of methanol and filtered through a 0.45 μm membrane filter. Then, a 20 μL aliquot was injected into the HPLC system (LC-2002; Jasco, Tokyo, Japan), which was equipped with a silica-based C18 reverse-phase column (5 μm, 4.6×150 mm; Phenomenex, Torrance, CA, USA), an RI detector (RI-2031, Jasco), and a UV light detector (UV-2075, Jasco). The mobile phase was methanol/water/acetic acid (90:5:5, v/v/v) and the flow rate was 1.0 mL/min. All peaks in the chromatograms corresponded to the retention times of internal standards such as erythorbic acid or myristic acid. The quantities of each substance

were determined by peak height at 265 nm using the Borwin software (v. 1.21, Jasco).

2.4. Purification and identification

Erythorbyl myristate was isolated from the reactant as previous described (Karmee, 2008; Park et al., 2011) with a slight modification. Briefly, immobilized lipase (Novozym 435®) was eliminated from the reactant by filtration using a glass filter. The filtrate was dissolved in 200 mL of *n*-hexane and the supernatant was discarded to eliminate residual myristic acid by centrifugation at 10,000×*g* for 15 min. The *n*-hexane was washed six times, and then the filtrate was dissolved in 200 mL of water. The supernatant was discarded to eliminate the residual erythorbic acid by centrifugation at 10,000×*g* for 20 min. This process was repeated six times.

To identify the purified product of lipase-catalyzed synthesis of erythorbyl myristate, LC electrospray ionization mass spectrometry (LC–ESI–MS) and two-dimensional correlated spectroscopy ^{1}H-nuclear magnetic resonance (2D-COSY ^{1}H-NMR) analyses were conducted. The product was separated using an LC system (Ultimate 3000 RS; Thermo Fisher Scientific, Massachusetts, CA, USA) equipped with a silica-based C18 reverse-phase column (1.7 μm, 100 Å, 2.1×150 mm; Phenomenex, Torrance, USA). Each

peak was analyzed using MS (LTQ; Thermo Fisher Scientific) and compared with the theoretical molecular weight of erythorbyl myristate. The site of esterification between erythorbic acid and myristic acid was determined using 2D-COSY ^{1}H-NMR (Advance 600; Bruker, Rheinstetten, Germany). The product was dissolved in dimethyl sulfoxide-d_6 (DMSO-d_6) with 0.03% tetramethylsilane (TMS). Chemical shift values are expressed in ppm relative to TMS.

2.5. Hydrophilic-lipophilic balance (HLB)

The value of HLB was used to quantify the preference of a surface-active agent between the water and oil phases, as described by Davies (Davies, 1957). Hydrophilic and lipophilic group numbers corresponding to the molecular structure of erythorbyl myristate were annotated and the HLB value of erythorbyl myristate was calculated as follows:

$$\mathrm{HLB} = \sum(h_i n_i) + \sum\left(l_j n_j\right) + 7$$

where h_i is the hydrophilic group number, l_j is the lipophilic group number, and n_i and n_j are the numbers of each group in the molecule.

2.6. *n*-Octanol-water partition coefficient (log *P*)

The value of log *P*, which quantifies the degree of lipophilicity of a substance, was determined using the atom/fragment contribution method (Meylan & Howard, 1995). The log *P* value was calculated by summing all atom/fragment contributions and a correction factor corresponding to the molecular structure of erythorbyl myristate, as follows:

$$\text{Log } P = \sum(f_i n_i) + \sum(c_j n_j) + 0.229$$

where f_i is the coefficient for each atom/fragment, c_j is the coefficient for each correction factor, and n_i and n_j are the numbers of each group for which the atom/fragment and correction factor corresponded to the molecular structure.

2.7. Isothermal titration calorimetry (ITC)

ITC (Affinity ITC; TA instrument, Delaware, USA) was used to determine critical micelle concentration (CMC) by measuring heats when micelles were demicellized (Loh, Brinatti, & Tam, 2016). ITC 20 mM erythorbyl myristate dissolved in distilled water containing 50% (v/v) dimethyl sulfoxide (DMSO)

was filtered using 0.45 μm syringe filter and was loaded to the injection syringe. Reference cell and sample cell were filled with 1.3 mL of distilled water and 1.3 mL of 50% (v/v) ethanol, respectively. The titration was carried out by injection of 5 μL sample from a 250 μL injection syringe into the sample cell after 5 min each injection at 25℃.

2.8. ABTS assay

The free radical scavenging activity of erythorbyl myristate was determined using the ABTS radical scavenging method (Re, Pellegrini, Proteggente, Pannala, Yang, & Rice-Evans, 1999) with a slight modification. A stock solution of 7.00 mM ABTS and 2.45 mM ammonium persulfate was stored in the dark for 12 h to produce ABTS radical ($ABTS^{\bullet+}$). Before the reaction, the solution was diluted with ethanol to adjust its absorbance to 0.70±0.05 at 734 nm. An erythorbyl myristate solution (50 μL) dissolved in DMSO was reacted with 200 μL of diluted ABTS solution in a Costar 3595 96-well plate (Corning Inc., Corning, NY, USA), and stored in the dark for 6 min. Then, absorbance was measured at 734 nm using plate reader (Multiskan™ GO, Thermo Fisher Scientific, Massachusetts, USA). ABTS radical scavenging activity was expressed as follows.

$$\text{ABTS radical scavenging activity} = 1 - \frac{(Sample\ absorbance)}{(Blank\ absorbance)} \times 100(\%)$$

2.9. DPPH assay

The DPPH assay was conducted as previously described (Reşat, Shela, Volker, Karen, Mustafa, & Kubilay, 2013) with a slight modification. We reacted 200 μL of 0.1 mM DPPH in ethanol with 50 μL of erythorbyl myristate solution in a 96-well plate, and stored the product in the dark for 30 min. After 30 min, absorbance was measured at 517 nm using plate reader (Multiskan™ GO, Thermo Fisher Scientific). DPPH radical scavenging activity was expressed as follows.

$$\text{DPPH radical scavenging activity} = 1 - \frac{(Sample\ absorbance)}{(Blank\ absorbance)} \times 100(\%)$$

2.10. Broth micro-dilution test and viable cell count

The antibacterial property of erythorbyl myristate against foodborne pathogens was evaluated using Gram-positive foodborne pathogen strains, including *Staphylococcus aureus* ATCC 12692, *S. aureus* ATCC 29213, *Bacillus cereus* ATCC 13061, and *B. cereus* ATCC 10876, and Gram-negative foodborne pathogen strains, including *Escherichia coli* ATCC

35150 and *Salmonella* Typhimurium ATCC 43971. The minimum inhibitory concentration (MIC) of erythorbyl myristate was determined using the broth micro-dilution method (Wiegand, Hilpert, & Hancock, 2008) with a slight modification. Sterile tryptic soy broth (TSB) (60 μL) was loaded into each well of a 96-well plate. Then, each well was inoculated with 100 μL of cell culture in TSB for a final concentration of 5×10^5 CFU/mL. Next, 40 μL of erythorbyl myristate solution dissolved in 5%(v/v) DMSO was mixed into the well. The 96-well plate was incubated in a plate reader (Multiskan GO; Thermo Fisher Scientific) measuring absorbance at 600 nm every 30 min at 37°C. The MIC was defined as the lowest concentration of erythorbyl myristate at which bacterial growth was fully inhibited after 12 h of incubation at 37°C (Nobmann, Bourke, Dunne, & Henehan, 2010). The minimum bactericidal concentration (MBC) of erythorbyl myristate was determined using viable cell count (Park, Lee, et al., 2018) with a slight modification. The MBC was defined as the lowest concentration of erythorbyl myristate at which viable cells were not detected. The erythorbyl myristate-treated cell cultures in TSB were incubated for 12 h at 37°C, and then inoculated to a tryptic soy agar plate. Colonies were counted after 12 h.

2.11. Transmission electron microscopy (TEM)

To prepare samples for TEM analysis, overnight cultures of *S. aureus* ATCC 12692 were treated with erythorbyl myristate dissolved in 5%(v/v) DMSO solution for 30 min at 37°C. Pellets were obtained from untreated and erythorbyl myristate-treated samples by centrifugation at 10,000×*g* for 10 min. The pellets were fixed overnight using modified Karnovsky's fixative, composed with 2% paraformaldehyde and 2% glutaraldehyde in 50 mM sodium cacodylate buffer (pH 7.2). Karnovsky's fixative was washed out with 50 mM sodium cacodylate buffer, and samples were post-fixed using 1% osmium tetroxide in 50 mM sodium cacodylate buffer for 2 h at 4°C and washed with distilled water at room temperature. Then, the samples were stained overnight using 0.5% uranyl acetate at 4°C, washed with distilled water, and dehydrated with increasing concentrations of ethanol (30, 50, 70, 80, 90, and 100%). After dehydration using 100% ethanol, the samples were treated with propylene oxide and infiltrated with Spurr's resin. The samples were dried overnight in an oven (60°C). Dried samples were analyzed by TEM (LIBRA 120; Carl Zeiss, Oberkochen, Germany) under standard conditions (Y.-H. Kim & Chung, 2011).

2.12. Statistical analysis

All data were analyzed using the SPSS software (ver. 25.0; SPSS, Chicago,

IL, USA) by analysis of variance and Duncan's multiple range test ($p < 0.05$). All data were obtained and processed from triplicate experiments.

3. Results and discussion

3.1. Lipase-catalyzed synthesis of erythorbyl myristate

Erythorbyl myristate was synthesized using immobilized lipase and GSL-MPS as shown in Fig. 1a. The process GSL-MPS was established for solvent-free synthesis of the erythorbyl fatty acid ester, in which the reactant was used as a reaction medium; this system allows much higher substrate concentrations. Hence, GSL-MPS has higher production yields than organic solvent systems (Yu, Lee, Shin, Park, & Chang, 2019). Several variables affect the efficiency of the enzyme reaction in GSL-MPS. First, the molar ratio of substrates is important, as many unreacted acyl donors (*e.g.*, myristic acid) can decrease production yield because the acyl acceptors (*e.g.*, erythorbic acid) are insufficient to maximize fatty acid ester production (H. Kim & Park, 2017). By contrast, lower amounts of acyl donors than acyl acceptors can lead to excessively high viscosity (Yu et al., 2019). Thus, it is necessary to determine the appropriate molar ratio between acyl donors and acyl acceptors. Enzyme concentration is another significant factor determining enzyme reaction efficiency. At low enzyme concentrations, large amounts of substrate remain available for the reaction, whereas at high concentrations, reaction efficiency is low. Therefore, in this study, we

adopted the molar ratio of erythorbic acid to myristic acid (1:2) and enzyme concentration (0.12 g/mL) from the GSL-MPS conditions of a previous study that optimized the reaction for erythorbyl laurate, which is similar to erythorbyl myristate (Yu et al., 2019). Under these conditions, esterification between the hydroxyl group (-OH) of erythorbic acid and carboxyl group (-COOH) of myristic acid was catalyzed by immobilized lipase (Novozym 435®) from *C. antarctica* (Fig. 1b).

(a)

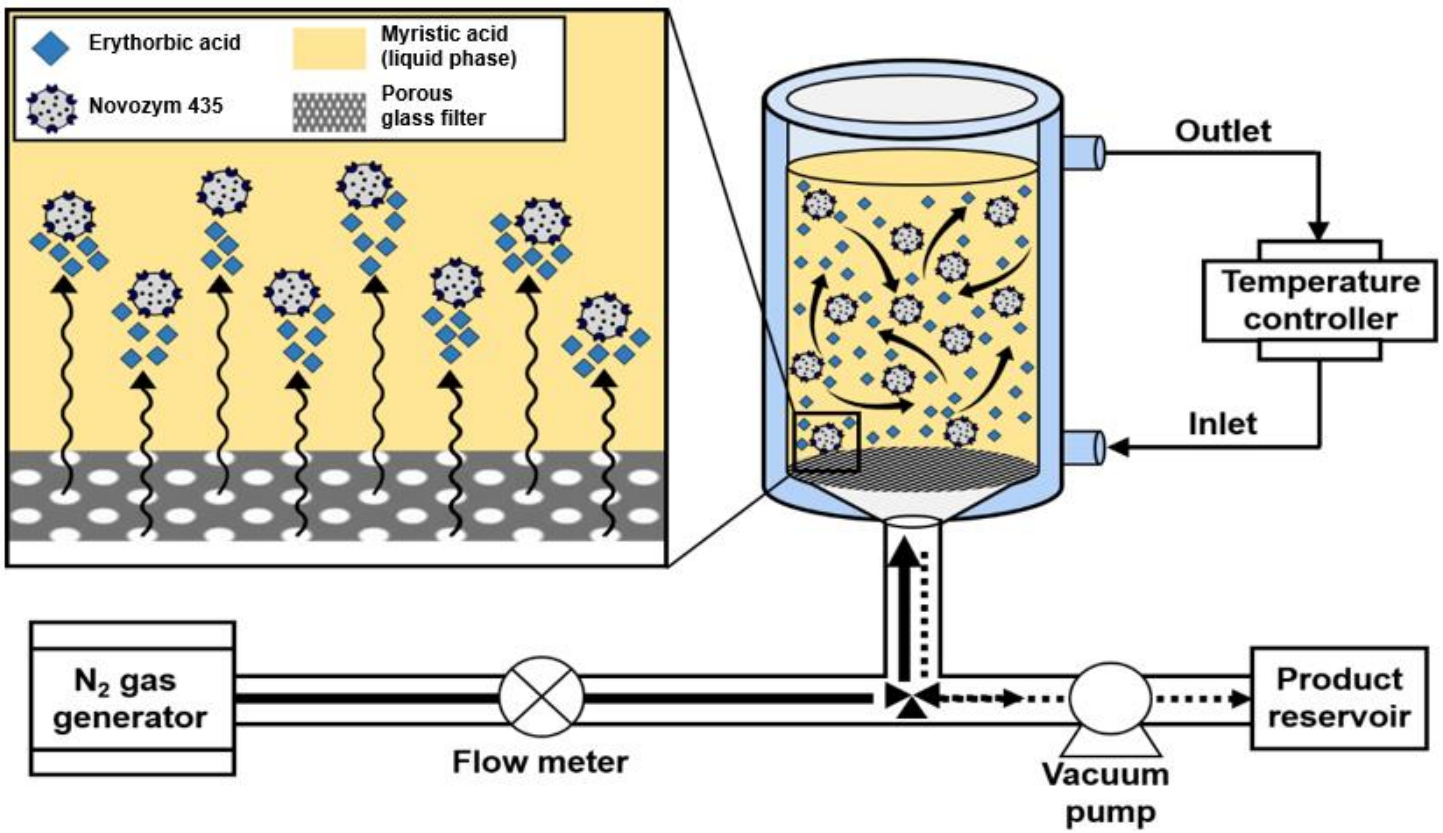
Erythorbic acid
Myristic acid (liquid phase)
Novozym 435
Porous glass filter
Outlet
Temperature controller
Inlet
N_2 gas generator
Flow meter
Vacuum pump
Product reservoir

(b)

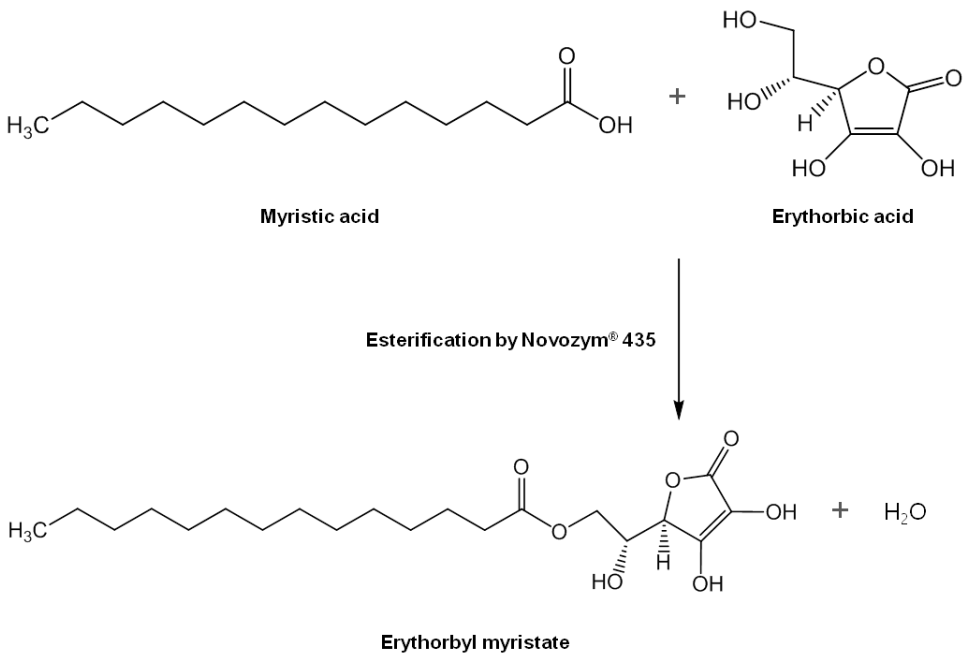

Fig. 1. Schematic representation of the lipase-catalyzed synthesis of erythorbyl myristate. (a) Gas–solid–liquid multiphase system for the solvent-free synthesis of erythorbyl myristate. (b) Lipase-catalyzed esterification between myristic acid and erythorbic acid.

During lipase-catalyzed esterification, the reactants were analyzed by HPLC equipped with UV and RI detectors. In the HPLC-UV chromatogram (Fig. 2a), peaks at 1.6 and 1.9 min were identified as erythorbic acid and debris of immobilized lipase, respectively, using internal standard compounds. Other peaks were not detected at 0 h, but were observed over time and expected as products synthesized as a result of esterification between erythorbic acid and myristic acid. In the previous study, synthesized erythorbyl laurate was observed early in the reaction (Park et al., 2011). Hence, a higher peak at 2.9 min was expected to represent erythorbyl myristate and another peak at 2.6 min may have indicated an unknown by-product of the reaction. In the HPLC-RI chromatogram (Fig. 2b), only one peak at 4.0 min was detected and identified as myristic acid using the internal standard compound. The peak height of erythorbyl myristate was converted into erythorbyl myristate concentration according to the calibration curve (Fig. 2c), and the final concentration, productivity, and yield of the reaction were calculated according to the time course of erythorbyl myristate production (Fig. 2d). The final concentration, productivity, and yield of erythorbyl myristate after 72 h of reaction were calculated as 119.45 mM, 1.99 mM/h, and 45.99 mg/mL myristic acid, respectively.

(a)

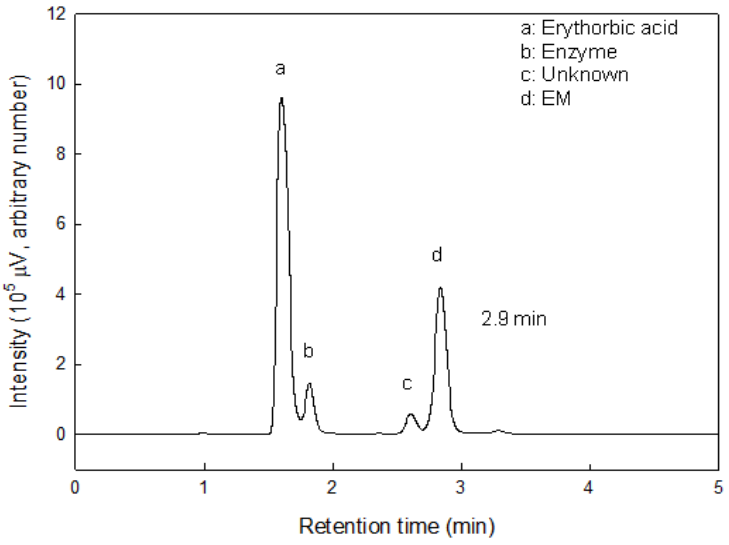
a: Erythorbic acid
b: Enzyme
c: Unknown
d: EM
a
b
c
d
2.9 min
Intensity (10^5 μV, arbitrary number)
Retention time (min)
0
2
4
6
8
10
12
0
1
2
3
4
5

(b)

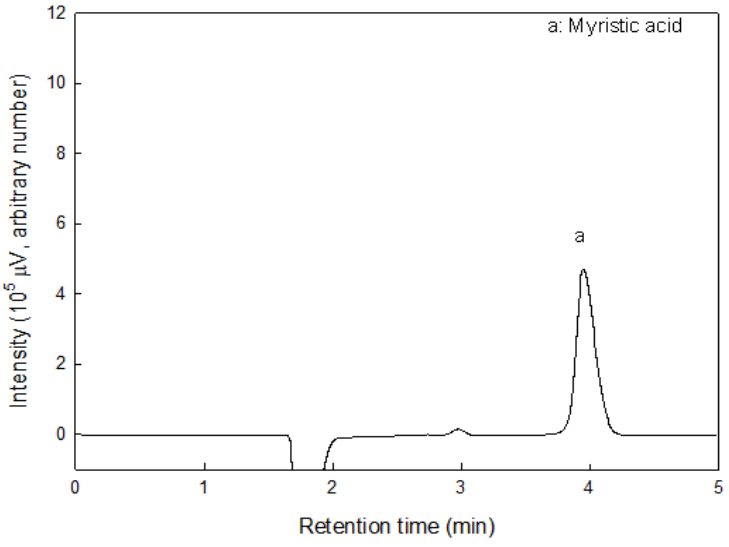
a: Myristic acid
a
Intensity (10^5 μV, arbitrary number)
Retention time (min)
0
2
4
6
8
10
12
0
1
2
3
4
5

(c)

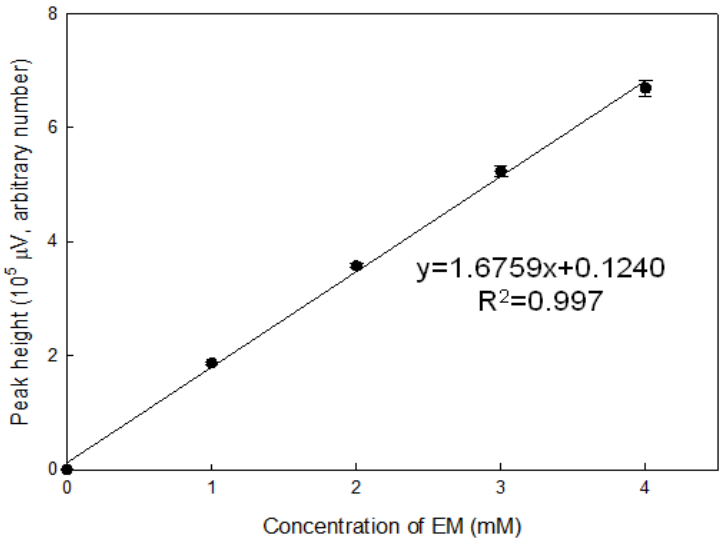
Peak height (10^5 μV, arbitrary number)
Concentration of EM (mM)
y=1.6759x+0.1240
R^2=0.997
0
2
4
6
8
0
1
2
3
4

(d)

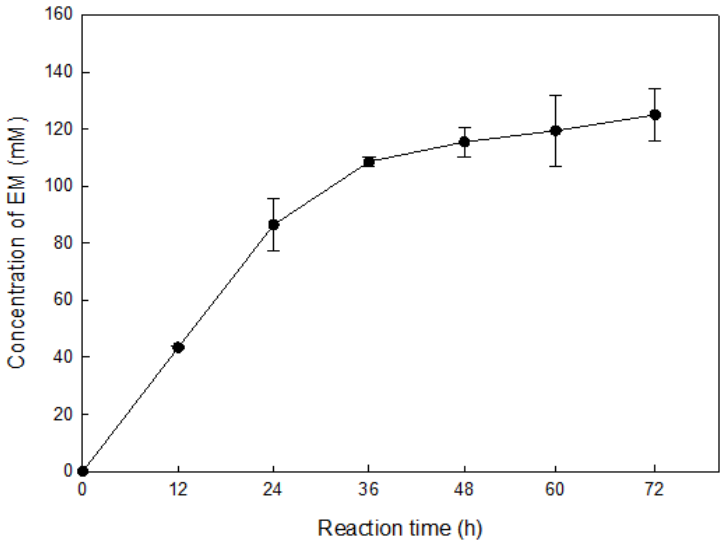
Concentration of EM (mM)
Reaction time (h)
0
20
40
60
80
100
120
140
160
0
12
24
36
48
60
72

Fig. 2. High-performance liquid chromatography–ultraviolet–refractive index (HPLC–UV/RI) analysis of the product after 72 h of lipase-catalyzed esterification between erythorbic acid and myristic acid. (a) HPLC chromatogram of the product obtained using a UV detector. (b) HPLC chromatogram of the product obtained using an RI detector. (c) Calibration curve of erythorbyl myristate concentration versus peak height at a retention time of 2.9 min in the HPLC chromatogram. (d) Time course of erythorbyl myristate synthesis.

3.2. Identification of erythorbyl myristate

After the reaction, the purified reactant was obtained by solvent extraction using *n*-hexane and water to eliminate myristic acid and erythorbic acid, respectively. HPLC analysis showed that the purified substance was detected at 2.9 min of retention time. Therefore, the purified substance was clearly erythorbyl myristate. However, for precise identification, further performed LC–ESI–MS and 2D-COSY ^{1}H-NMR analyses of erythorbyl myristate was conducted.

The molecular weight of the purified substance was determined by LC–ESI–MS. From the LC chromatogram, we detected a single peak at 2.9 min of retention time (Fig. 3a), similar to the result shown in Fig. 2a. We analyzed this peak by ESI–MS, in full scan mode with the negative ion setting. The mass spectra showed a molecular ion at *m/z* = 384.0 $[M\text{-}H]^-$ and 767.5 $[2M\text{-}H]^-$, corresponding to the theoretical molecular weight (386.48) of erythorbyl myristate (Fig. 3b).

The LC–ESI–MS results demonstrated that esterification between erythorbic acid and myristic acid had occurred, but could not reveal the exact site of esterification. Previous studies have shown that the carboxyl group of myristic acid was esterified with the hydroxyl group of erythorbic acid at C-6 (Park et al., 2011; Sun et al., 2013). Therefore, each proton in the ^{1}H-NMR

spectrum was annotated as a number based on these studies, and 2D-COSY ^{1}H-NMR was conducted to identify proton coupling. The 2D-COSY ^{1}H-NMR spectrum (Fig. 3c) showed that proton coupling had occurred between nearby protons; coupling signals were observed in a symmetrical position relative to the diagonal. We observed four significant couplings; notably, peaks 5 and 6 were coupled with peaks 9 and 8, respectively. These proton couplings were consistent with previous ^{1}H-NMR results for other erythorbyl fatty acid esters. Therefore, the site of esterification in erythorbyl myristate was verified to be C-6 of erythorbic acid.

(a)

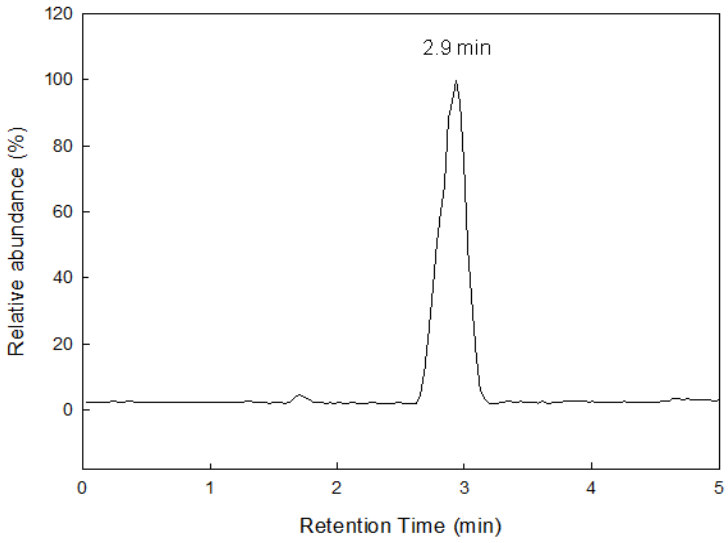
2.9 min
Relative abundance (%)
Retention Time (min)
0
20
40
60
80
100
120
0
1
2
3
4
5

(b)

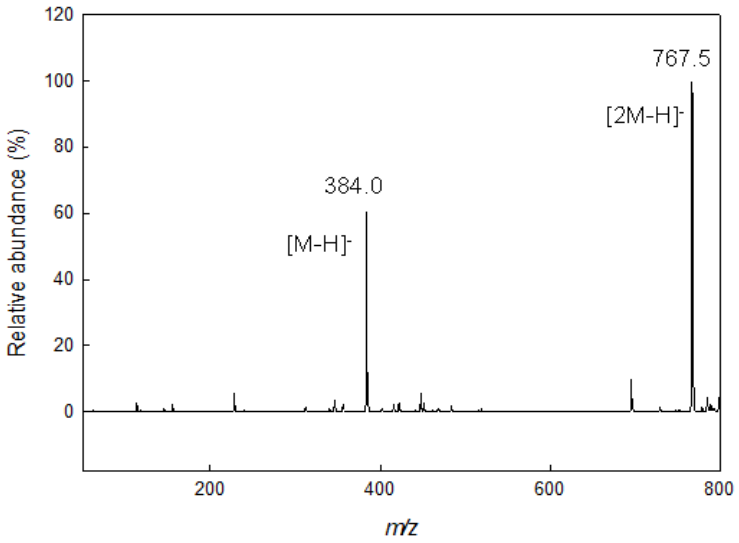
767.5
[2M-H]-
384.0
[M-H]-
Relative abundance (%)
m/z
0
20
40
60
80
100
120
200
400
600
800

(c)

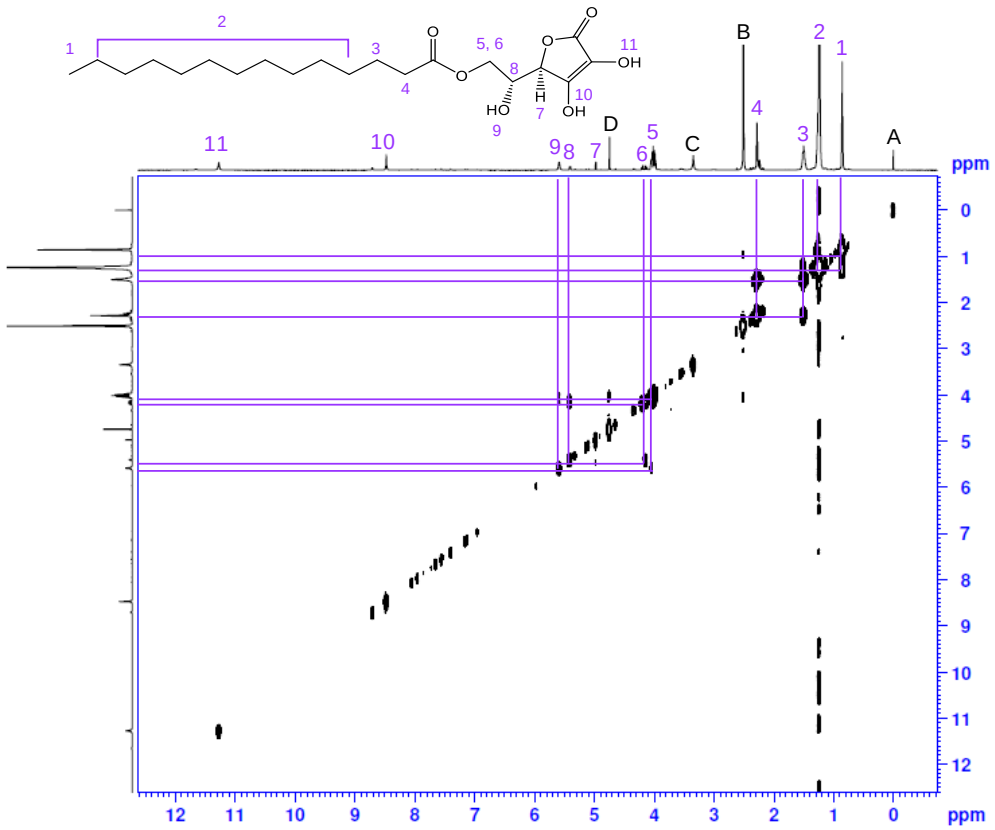

Fig. 3. Liquid chromatography–electrospray ionization–mass spectrometry (LC–ESI–MS) and protein nuclear magnetic resonance (^{1}H-NMR) analyses of the product from lipase-catalyzed synthesis of erythorbyl myristate. (a) LC chromatogram of purified erythorbyl myristate obtained using an ultraviolet detector. (b) Mass spectrum of the peak at 2.9 min retention time in the LC chromatogram. (c) Two-dimensional correlation spectrometry ^{1}H-

NMR spectrum of purified erythorbyl myristate. A: tetramethylsilane; B: dimethyl sulfoxide-d_6; C: H_2O; D: D_2O.

3.3. Emulsifying property of erythorbyl myristate

The physico-structural characteristics of erythorbyl myristate were evaluated to calculate the HLB and log *P*. Appropriate conditions are required for emulsification; these are determined by the hydrophilic and hydrophobic moieties of the emulsifier. For example, Tween emulsifiers have different hydrophobic moieties according to their fatty acid chain length, which lead to different emulsifying properties. Therefore, we calculated the ratio of the hydrophilic and hydrophobic moieties of erythorbyl myristate to determine the optimal conditions for its emulsification.

Hydrophilic and lipophilic groups in the erythorbyl myristate structure are shown in Fig. 4a and Table 1. Log *P* values for the atoms/fragments of the structure are shown in Fig. 4b and Table 2. The HLB value of erythorbyl myristate was 11.5; substances with an HLB value between 8 and 11 are generally used for O/W emulsion. Therefore, erythorbyl myristate is expected to be a stable emulsifier for O/W emulsion. The log *P* value of erythorbyl myristate was 5.02. A negative log *P* value of a compound indicates hydrophilicity (*e.g.*, log *P* values of DMSO and methanol are −1.3 and −0.76, respectively), whereas positive log *P* indicates that a compound is hydrophobic (*e.g.*, log *P* values of octane and decane are 5.2 and 5.8, respectively). Therefore, erythorbyl myristate is expected to be suitable for

O/W emulsion with high hydrophobicity.

The ITC thermogram of erythorbyl myristate is shown in Fig. 5. As titration was progressed, ΔH was decreased and reached saturation. it can be divided into two different concentration regions based on the CMC. When the concentration of erythorbyl myristate is lower than the CMC, ΔH was measured from both demicellization and dilution effect. Whereas the concentration of erythorbyl myristate exceeding the CMC, ΔH was measured from only dilution effect (Dai & Tam, 2003). CMC of erythorbyl myristate expressed as the intersection of the two regions is 0.33 mM. Overall the results of HLB, log *P*, and CMC, erythorbyl myristate could be utilized as an emulsifier in the O/W emulsion with high hydrophobicity.

(a)

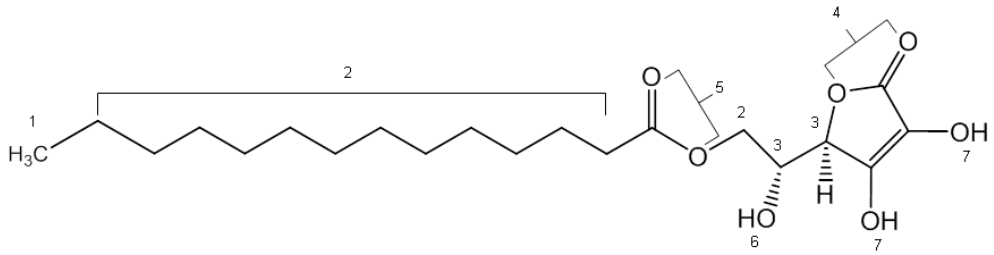

(b)

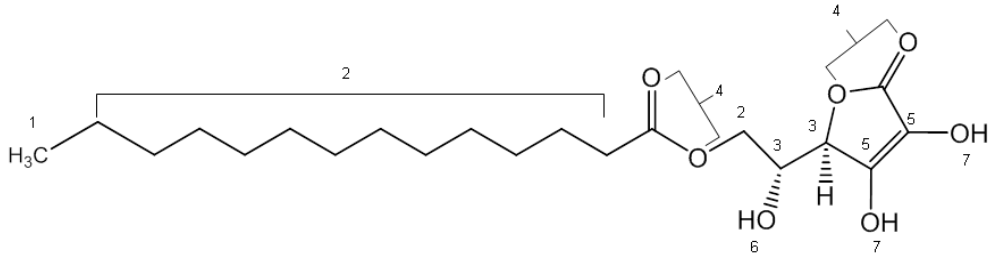

Fig. 4. Molecular diagrams of erythorbyl myristate structure used to calculate emulsifying properties including (a) the hydrophilic–lipophilic balance based on the Davies method and (b) the *n*-octanol/water partition coefficient (log *P*) based on the atom/fragment contribution method.

.

Table 1. Lipophilic and hydrophilic groups of erythorbyl myristate used to calculate the hydrophilic–lipophilic balance

Number	Lipophilic groups (i)	Group number (l)	Frequency (n)
1	CH_3-		1
2	-CH-	-0.475	13
3	=CH-		2
	Hydrophilic groups (j)	Group number (h)	Frequency (n)
4	Ester (sorbitan ring)	6.8	1
5	Ester (free)	2.4	1
6	Hydroxyl (free)	1.9	1
7	Hydroxyl (sorbitan ring)	0.5	2

Table 2. Fragments and correction factors of erythorbyl myristate used to calculate the *n*-octanol/water partition coefficient

Number	Fragments (i)	Coefficiency (f)	Frequency (n)
1	-CH_3	0.5473	1
2	-CH_2-	0.4911	13
3	-CH-	-1.4086	1
4	-C(=O)O	-0.8855	2
5	=C- or =C<	0.3614	2
6	-OH (aliphatic attachment)	0.3836	2
7	-OH (olefinic attachment)	-0.9505	2
	Correction factors (j)	Coefficiency (c)	Frequency (n)
	Cyclic ester	-1.0577	1
	More than one aliphatic –OH	0.4064	1
	HO-C=C(-OH)-C(=O)-O- (cyclic)	2.1000	1

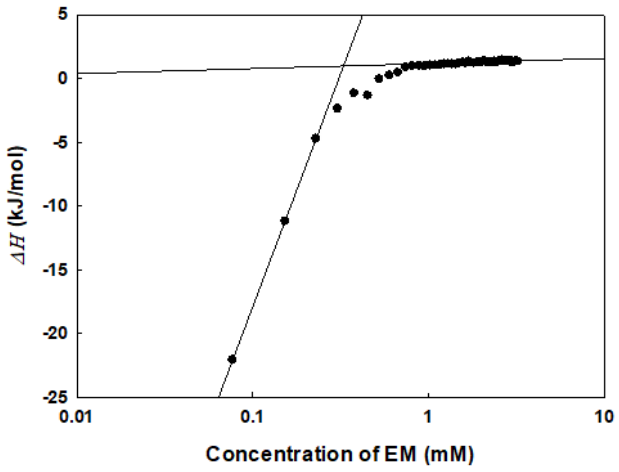

Fig. 5. Calorimetric titration thermogram of 20 mM erythorbyl myristate in 50% ethanol at 25°C. EM: erythorbyl myristate.

3.4. Antioxidative property of erythorbyl myristate

The free radical scavenging activity of erythorbyl myristate was evaluated using ABTS and DPPH assays. The ABTS assay results are shown in Fig. 6a. The two substrates of erythorbyl myristate, erythorbic acid and myristic acid, were also analyzed to determine whether the antioxidative property resulted from the hydrophilic moiety (*i.e.,* erythorbic acid). The ABTS radical scavenging activities of erythorbyl myristate were 4.88, 20.82, 36.77, 57.64, 75.25, and 85.65% at erythorbyl myristate concentrations of 10, 20, 30, 40, 50, and 60 μM, respectively. The half-maximal effective concentration (EC_{50}) of erythorbyl myristate and erythorbic acid were 34.43 and 27.24 μM, respectively.

The DPPH assay results for erythorbyl myristate, erythorbic acid, and myristic acid are shown in Fig. 6b. The DPPH radical scavenging activities of erythorbyl myristate increased with concentration, with activities of 7.40, 22.49, 39.45, 58.07, 73.09, and 84.53% at erythorbyl myristate concentrations of 10, 20, 30, 40, 50, and 60 μM, respectively. The EC_{50} values of erythorbyl myristate and erythorbic acid were 35.77 and 38.2 μM, respectively. The antioxidative property of erythorbyl myristate was contributed by erythorbic acid, as was previously reported for erythorbyl

laurate (Park et al., 2017). However, myristic acid showed no antioxidative effect on ABTS and DPPH radicals. Erythorbic acid inhibited lipid oxidation in the emulsion (Park et al., 2017). Together, these results show that erythorbyl myristate efficiently retards rancidification by scavenging free radical from lipids in emulsion-based foods.

(a)

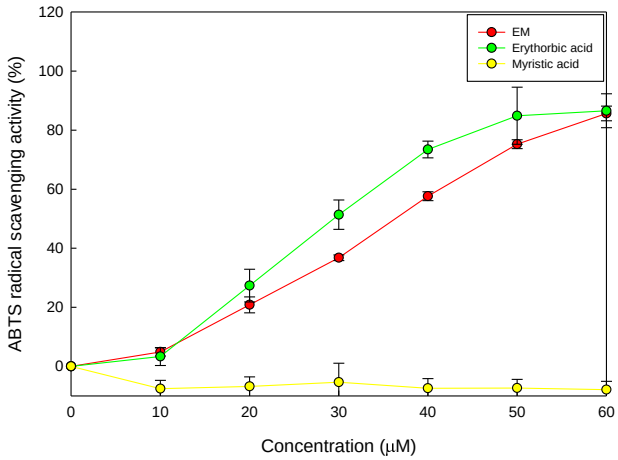

(b)

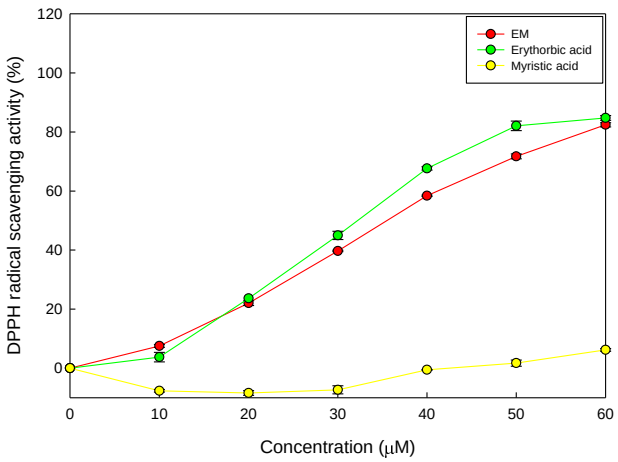

Fig. 6. Antioxidative property of erythorbyl myristate based on radical scavenging activity. (a) 2,2'-azino-bis (3-ethylbenzothiazoline-6-sulfonic acid) (ABTS) and (b) 2,2-diphenyl-1-picryl-hydrazyl-hydrate (DPPH)

radical scavenging activity of erythorbyl myristate. EM: erythorbyl myristate.

3.5. Antibacterial property of erythorbyl myristate

Erythorbyl myristate exerted bacteriostatic and bactericidal activities against the Gram-positive foodborne pathogens *S. aureus* and *B. cereus*. In the broth micro-dilution test, pathogens were treated with various concentrations of erythorbyl myristate, and cell growth was observed via increased absorbance at 600 nm (Fig. 7a, 7b, 7c, and 7d). Bacterial growth patterns differed according to the concentration of erythorbyl myristate, and the MICs of each pathogen were calculated from these results. Bactericidal activity was evaluated in erythorbyl myristate in terms of MBC by counting viable cells (Fig. 7e, 7f, 7g, and 7h and Table 3). Growth curves for all Gram-positive foodborne pathogens exhibited an increase in lag time (λ) coinciding with a decrease in the maximum specific growth rate (μ_{max}) as erythorbyl myristate concentration increased. However, the Gram-negative foodborne pathogens *E. coli* and *S.* Typhimurium showed no bacteriostatic (Fig. 8a and 8b) or bactericidal (Fig. 8c and 8d) activity. Therefore, erythorbyl myristate showed antibacterial property against only Gram-positive pathogens; a similar result was previously obtained for erythorbyl laurate, which cannot penetrate the lipopolysaccharide layer of Gram-negative pathogens (Park, Jo, et al., 2018).

The antibacterial mechanism of erythorbyl myristate was revealed by

TEM analysis (Fig. 9). In untreated *S. aureus* ATCC 12692, intact cytoplasmic membrane was observed, whereas MIC erythorbyl myristate-treated *S. aureus* ATCC 12692 showed a loss of cell contents and significant convolution of the cytoplasmic membrane. Consequently, full loss of cell contents was observed for *S. aureus* treated with 2 times the MIC of erythorbyl myristate. TEM analysis suggested that the mechanism of the antibacterial property of erythorbyl myristate was alteration of membrane permeability. The erythorbyl fatty acid ester, which is a non-ionic emulsifier, attached to the hydrophilic surface of the cytoplasmic membrane (Fig. 10). The attached erythorbyl fatty acid ester was inserted into the membrane by hydrophobic interaction, where it depolarized and disrupted the permeability of the membrane (Park, Jo, et al., 2018).

(a)

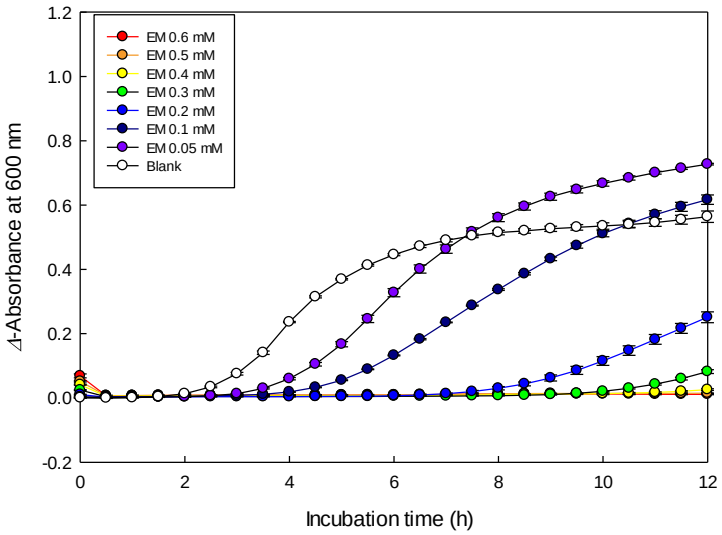
EM 0.6 mM
EM 0.5 mM
EM 0.4 mM
EM 0.3 mM
EM 0.2 mM
EM 0.1 mM
EM 0.05 mM
Blank
Δ-Absorbance at 600 nm
Incubation time (h)

(b)

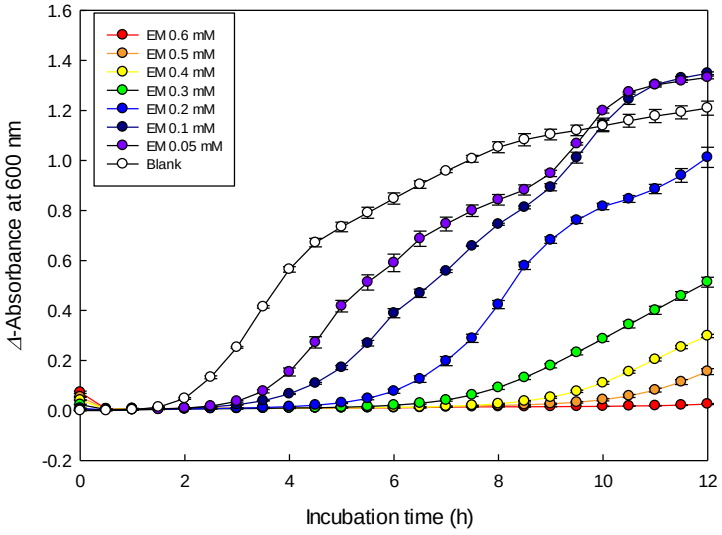
EM 0.6 mM
EM 0.5 mM
EM 0.4 mM
EM 0.3 mM
EM 0.2 mM
EM 0.1 mM
EM 0.05 mM
Blank
Δ-Absorbance at 600 nm
Incubation time (h)

(c)

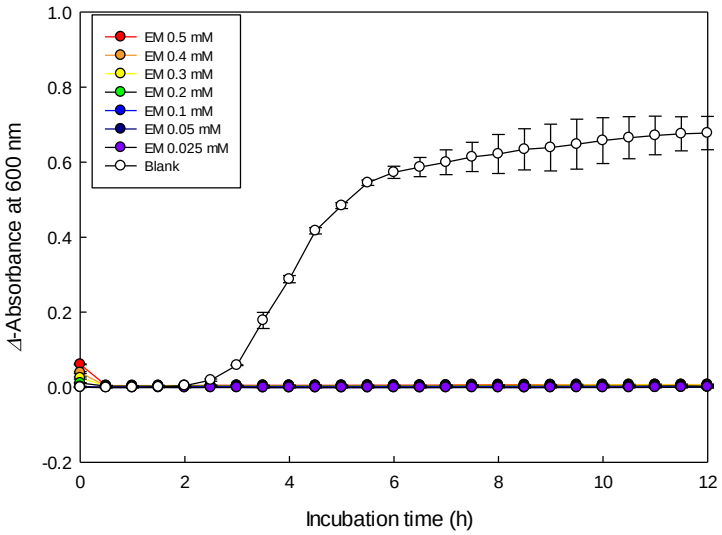
EM 0.5 mM
EM 0.4 mM
EM 0.3 mM
EM 0.2 mM
EM 0.1 mM
EM 0.05 mM
EM 0.025 mM
Blank
Δ1-Absorbance at 600 nm
Incubation time (h)
1.0
0.8
0.6
0.4
0.2
0.0
-0.2
0
2
4
6
8
10
12

(d)

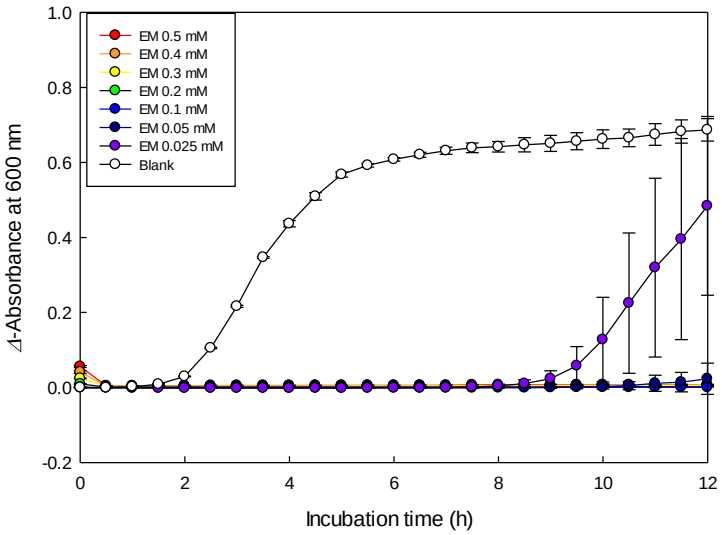
EM 0.5 mM
EM 0.4 mM
EM 0.3 mM
EM 0.2 mM
EM 0.1 mM
EM 0.05 mM
EM 0.025 mM
Blank
Δ1-Absorbance at 600 nm
Incubation time (h)
1.0
0.8
0.6
0.4
0.2
0.0
-0.2
0
2
4
6
8
10
12

(e)

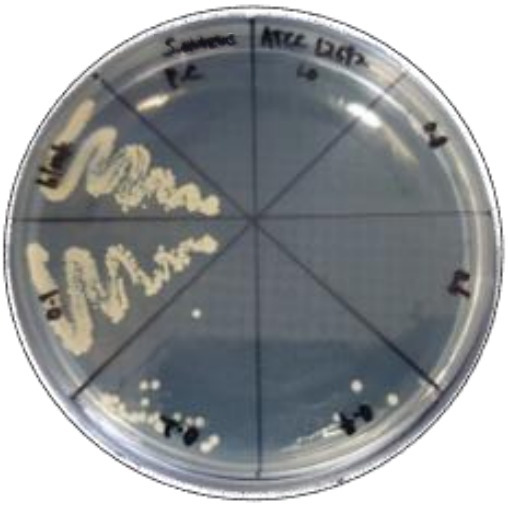

(f)

(g)

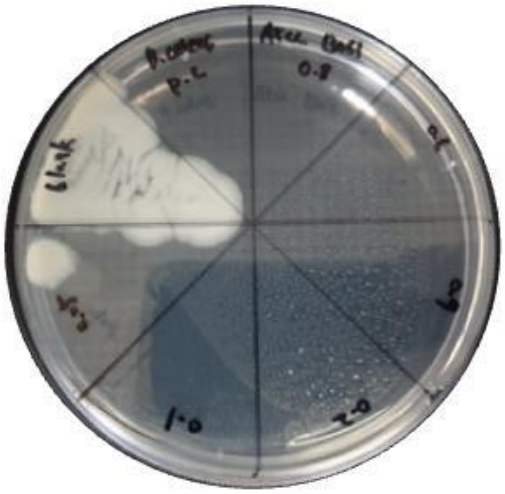

(h)

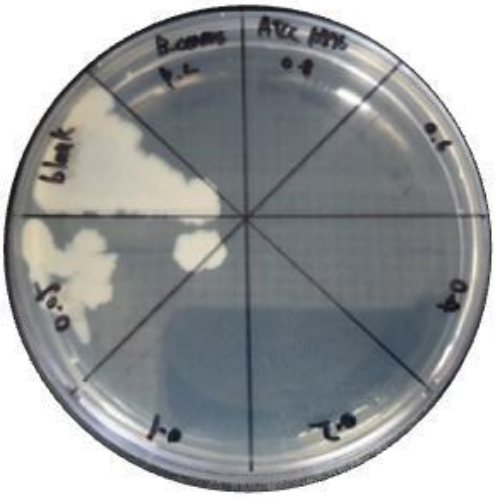

Fig. 7. Bacteriostatic and bactericidal activities of erythorbyl myristate against Gram-positive pathogens. Growth curves of (a) *Staphylococcus aureus* ATCC 12692 and (b) *S. aureus* ATCC 29213 treated with 0.05–0.60 mM erythorbyl myristate. Growth curves of (c) *Bacillus cereus* ATCC 13061 and (d) *B. cereus* ATCC 10876 treated with 0.025–0.50 mM erythorbyl myristate. Viable cell counts of (e) *S. aureus* ATCC 12692 and (f) *S. aureus* ATCC 29213 treated with 0.01–1.00 mM erythorbyl myristate. Viable cell counts of (g) *B. cereus* ATCC 13061 and (h) *B. cereus* ATCC 10876 treated with 0.05–0.80 mM erythorbyl myristate. EM: erythorbyl myristate.

Table 3. Bacteriostatic and bactericidal activities of erythorbyl myristate against Gram-positive pathogens

Bacterial strains	MIC[1] (mM)	MBC[2] (mM)	Concentration[3] (mM)	λ[4] (h)	μ_{max}[5] (OD_{600}/h^{-1})
Staphylococcus aureus ATCC 12692	0.60±0.00	0.73±0.12	0.40	9.17±0.29^{c}	0.015±0.001^{c}
			0.20	4.83±0.58^{b}	0.069±0.003^{a}
			Blank	1.50±0.00^{a}	0.191±0.014^{b}
Staphylococcus aureus ATCC 29213	0.60±0.00	0.93±0.12	0.40	3.67±0.58^{b}	0.099±0.001^{a}
			0.20	4.67±0.29^{c}	0.311±0.004^{b}
			Blank	1.00±0.00^{a}	0.324±0.014^{b}
Bacillus cereus ATCC 10876	0.07±0.03	0.08±0.03	0.050	10.5±1.80^{c}	0.018±0.031^{a}
			0.025	6.33±1.26^{b}	0.195±0.154^{ab}
			Blank	1.50±0.00^{a}	0.261±0.008^{b}
Bacillus cereus ATCC 13061	0.06±0.04	0.07±0.03	0.050	11.5±0.87^{b}	0.001±0.001^{a}
			0.025	11.5±0.50^{b}	0.004±0.004^{a}
			Blank	2.00±0.00^{a}	0.259±0.003^{b}

1) Minimum inhibitory concentration, 2) minimum bactericidal concentration, 3) sub-MIC concentration, 4) lag time, 5) maximum specific growth rate.

[a-c] Means in the same column of each strain with different superscripts differ significantly ($p < 0.05$, Duncan's multiple range test).

(a)

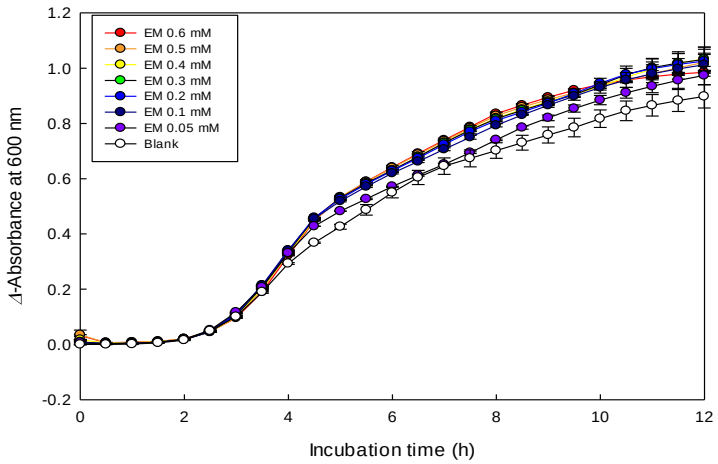
EM 0.6 mM
EM 0.5 mM
EM 0.4 mM
EM 0.3 mM
EM 0.2 mM
EM 0.1 mM
EM 0.05 mM
Blank
Δ1-Absorbance at 600 nm
Incubation time (h)

(b)

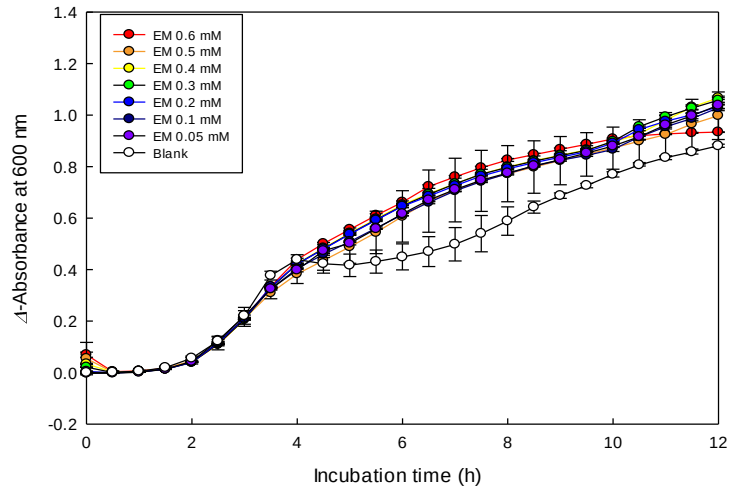
EM 0.6 mM
EM 0.5 mM
EM 0.4 mM
EM 0.3 mM
EM 0.2 mM
EM 0.1 mM
EM 0.05 mM
Blank
Δ1-Absorbance at 600 nm
Incubation time (h)

(c)

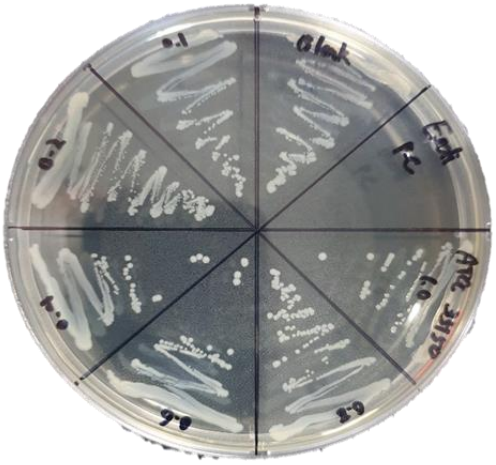

(d)

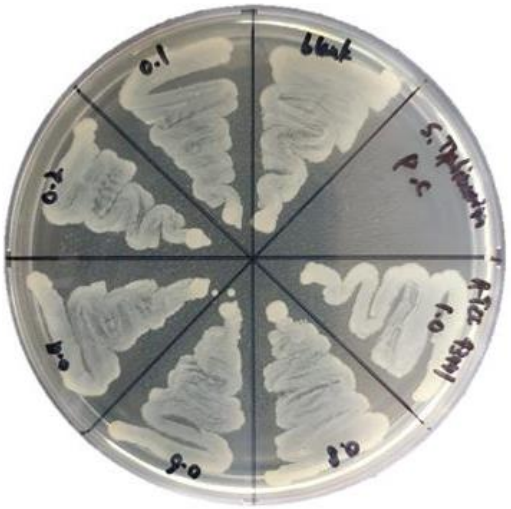

Fig. 8. Bacteriostatic and bactericidal activities of erythorbyl myristate against Gram-negative pathogens. Growth curves of (a) *Escherichia coli* ATCC 35150 and (b) *Salmonella* Typhimurium ATCC 43971 treated with 0.05–0.60 mM erythorbyl myristate. Viable cell counts of (c) *E. coli* ATCC 35150 and *S.* Typhimurium ATCC 43971 treated with 0.01–1.0 mM erythorbyl myristate. EM: erythorbyl myristate.

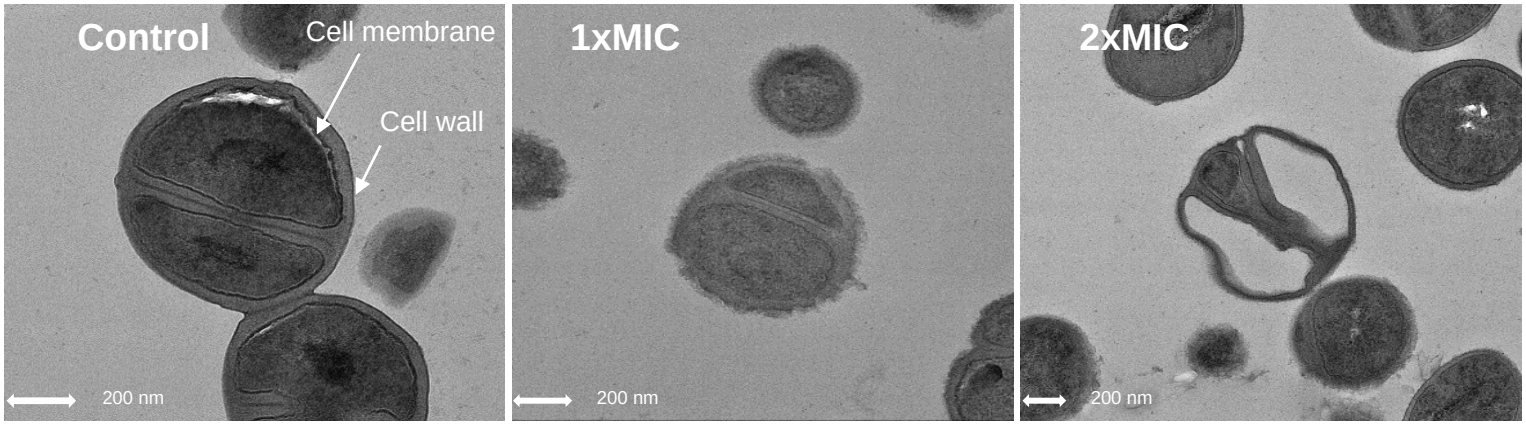

Fig. 9. Transmission electron micrograph of *Staphylococcus aureus* ATCC 12692 treated with the minimum inhibitory concentration (MIC) and 2×MIC of erythorbyl myristate.

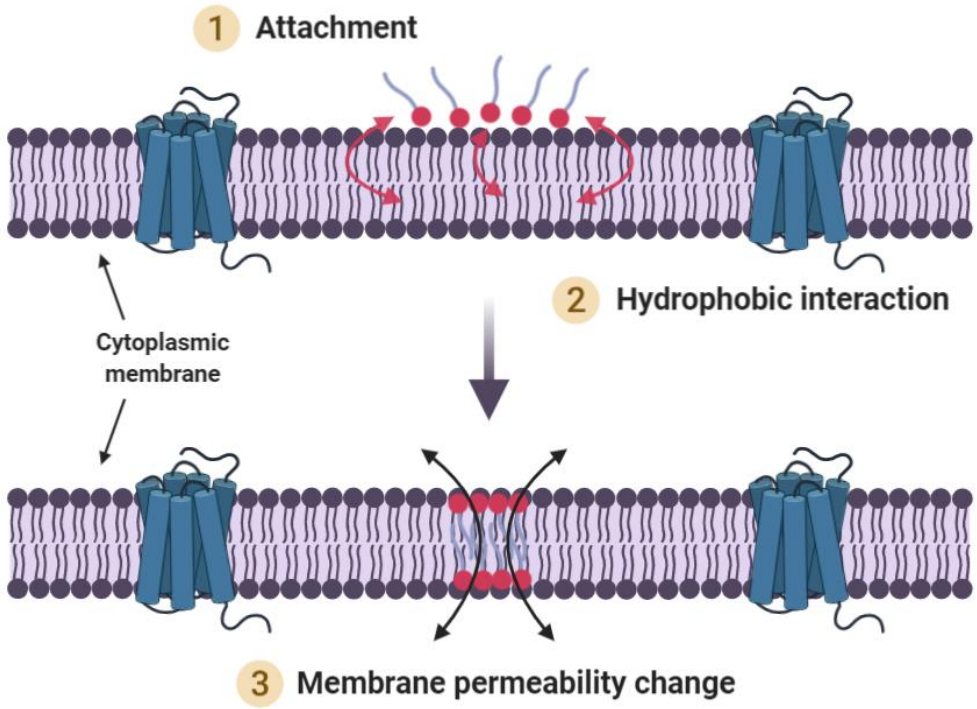

Fig. 10. The putative mode of action of erythorbyl myristate targeting the cytoplasmic membrane of Gram-positive pathogens.

4. Conclusions

In this study, a novel multi-functional emulsifier with antioxidative and antibacterial properties was successfully produced using immobilized lipase and GSL-MPS. After purification, the reaction product was identified as erythorbyl myristate using LC–ESI–MS and 2D-COSY ^{1}H-NMR. The multi-functionality of erythorbyl myristate was evaluated in terms of terms of its emulsifying, antioxidative, and antibacterial properties. Together, these results suggest that erythorbyl myristate is a multi-functional antioxidative and antibacterial emulsifier that may be used in O/W emulsion-based foods with high hydrophobicity. Furthermore, changing the hydrophobic moiety of erythorbyl myristate by altering fatty acid chains is expected to produce a range of emulsifiers, each with its own optimal conditions for emulsification. We propose that erythorbyl myristate is suitable for use as a multi-functional emulsifier to enhance the quality and safety of emulsion-based foods.

5. References

Chen, G., & Tao, D. (2005). An experimental study of stability of oil-water emulsion. *Fuel Processing Technology, 86*, 499-508.

Dai, S., & Tam, K. C. (2003). Isothermal titration calorimetric studies of alkyl phenol ethoxylate surfactants in aqueous solutions. *Colloids and Surfaces A: Physicochemical and Engineering Aspects, 229*(1), 157-168.

Davies, J. T. (1957). A quantitative kinetic theory of emulsion type, I. physical chemistry of the emulsifying agent. *Gas/Liquid and Liquid/Liquid Interfaces. In: Proceedings of 2nd International Congress Surface Activity, 1*, 426-438.

Frankel, E. N. (1984). Chemistry of free radical and singlet oxidation of lipids. *Progress in Lipid Research, 23*(4), 197-221.

Kabara, J. J., Swieczkowski, D. M., Conley, A. J., & Truant, J. P. (1972). Fatty acids and derivatives as antimicrobial agents. *Antimicrobial Agents and Chemotherapy, 2*(1), 23-28.

Karmee, S. K. (2008). Lipase catalyzed synthesis of ester-based surfactants from biomass derivatives. *Biofuels, Bioproducts and Biorefining, 2*(2), 144-154.

Kim, H., & Park, C. (2017). Enzymatic synthesis of phenethyl ester from phenethyl alcohol with acyl donors. *Enzyme and Microbial Technology, 100*, 37-43.

Kim, Y.-H., & Chung, H.-J. (2011). The effects of Korean propolis against foodborne pathogens and transmission electron microscopic examination. *New Biotechnology, 28*(6), 713-718.

Loh, W., Brinatti, C., & Tam, K. C. (2016). Use of isothermal titration calorimetry to study surfactant aggregation in colloidal systems. *Biochimica et Biophysica Acta (BBA) - General Subjects, 1860*(5), 999-1016.

Luther, M., Parry, J., Moore, J., Meng, J., Zhang, Y., Cheng, Z., & Yu, L. (2007). Inhibitory effect of Chardonnay and black raspberry seed extracts on lipid oxidation in fish oil and their radical scavenging and antimicrobial properties. *Food Chemistry, 104*(3), 1065-1073.

Maijala, R., Lyytikäinen, O., Johansson, T., Autio, T., Aalto, T., Haavisto, L., & Honkanen-Buzalski, T. (2001). Exposure of *Listeria monocytogenes* within an epidemic caused by butter in Finland. *International Journal of Food Microbiology, 70*(1), 97-109.

Meylan, W. M., & Howard, P. H. (1995). Atom/fragment contribution method for estimating octanol–water partition coefficients. *Journal of*

Pharmaceutical Sciences, 84(1), 83-92.

Nobmann, P., Bourke, P., Dunne, J., & Henehan, G. (2010). *In vitro* antimicrobial activity and mechanism of action of novel carbohydrate fatty acid derivatives against *Staphylococcus aureus* and MRSA. *Journal of Applied Microbiology, 108*(6), 2152-2161.

Park, K.-M., Jo, S.-K., Yu, H., Park, J.-Y., Choi, S. J., Lee, C. J., & Chang, P.-S. (2018). Erythorbyl laurate as a potential food additive with multi-functionalities: Antibacterial activity and mode of action. *Food Control, 86*, 138-145.

Park, K.-M., Lee, D. E., Sung, H., Lee, J., & Chang, P.-S. (2011). Lipase-catalysed synthesis of erythorbyl laurate in acetonitrile. *Food Chemistry, 129*(1), 59-63.

Park, K.-M., Lee, M. J., Jo, S.-K., Choi, S. J., Lee, J., & Chang, P.-S. (2017). Erythorbyl laurate as a potential food additive with multi-functionalities: Interfacial characteristics and antioxidant activity. *Food Chemistry, 215*, 101-107.

Park, K.-M., Lee, S. J., Yu, H., Park, J.-Y., Jung, H.-S., Kim, K. , & Chang, P.-S. (2018). Hydrophilic and lipophilic characteristics of non-fatty acid moieties: Significant factors affecting antibacterial activity of lauric acid esters. *Food Science and Biotechnology, 27*(2), 401-409.

Re, R., Pellegrini, N., Proteggente, A., Pannala, A., Yang, M., & Rice-Evans, C. (1999). Antioxidant activity applying an improved ABTS radical cation decolorization assay. *Free Radical Biology and Medicine, 26*(9), 1231-1237.

Reşat, A., Shela, G., Volker, B., Karen, M. S., Mustafa, Ö., & Kubilay, G. (2013). Methods of measurement and evaluation of natural antioxidant capacity/activity (IUPAC Technical Report). *Pure and Applied Chemistry, 85*(5), 957-998.

Shahidi, F., & Zhong, Y. (2010). Lipid oxidation and improving the oxidative stability. *Chemical Society Reviews, 39*(11), 4067-4079.

Sun, W.-J., Zhao, H.-X., Cui, F.-J., Li, Y.-H., Yu, S.-L., Zhou, Q. , & Dong, Y. (2013). D-isoascorbyl palmitate: lipase-catalyzed synthesis, structural characterization and process optimization using response surface methodology. *Chemistry Central Journal, 7*(1), 114-126.

Wiegand, I., Hilpert, K., & Hancock, R. E. W. (2008). Agar and broth dilution methods to determine the minimal inhibitory concentration (MIC) of antimicrobial substances. *Nature Protocols, 3*(2), 163-175.

Yang, J., Jiang, B., He, W., & Xia, Y.-M. (2012). Hydrophobically modified alginate for emulsion of oil in water. *Carbohydrate Polymers, 87*, 1503-1506.

Yu, H., Lee, M.-W., Shin, H., Park, K.-M., & Chang, P.-S. (2019). Lipase-catalyzed solvent-free synthesis of erythorbyl laurate in a gas-solid-liquid multiphase system. *Food Chemistry, 271*, 445-449.

Yuan, Y., Gao, Y., Mao, L., & Zhao, J. (2008). Optimization of condition for the preparation of β-carotene nanoemulsions using response surface methodology. *Food Chemistry, 107*, 1300-1306.

Zhang, S., Zhang, M., Fang, Z., & Liu, Y. (2017). Preparation and characterization of blended cloves/cinnamon essential oil nanoemulsions. *Lebensmittel-Wissenschaft & Technologie*, *75*, 316-322.

국문초록

본 논문에서는 항산화와 항균능을 가진 다기능성 유화제로 이용이 기대되는 에리소르빌 미리스테이트(erythorbyl myristate)를 고정화 라이페이스를 이용하여 에리소르빈산과 미리스트산 간의 효소적 에스터화 반응을 통해 합성하였다. LC-ESI-MS와 2D-COSY ^{1}H-NMR 분석을 통해 반응생성물의 구조가 6-*O*-myristoyl-erythorbic acid임을 확인하였다. 에리소르빌 미리스테이트의 다기능성은 유화능, 항산화능, 항균능에 대하여 평가되었다. 유화능의 경우, 에리소르빌 미리스테이트의 분자구조로부터 hydrophilic-lipophilic balance (11.5)와 log *P* (5.02)를 계산하였고, 등온열량측정기(ITC)를 통해 CMC (0.33 mM)을 측정하였다. 이러한 수치들은 에리소르빌 미리스테이트이 소수성 특성이 높은 수중유적형 에멀젼을 형성할 수 있음을 보여준다. 항산화능의 경우, ABTS assay와 DPPH assay를 통해 에리소르빌 미리스테이트의 라디칼 소거능으로써 평가하였다. 에리소르빌

미리스테이트의 라디칼 소거능은 에리소르빈산으로부터 유래하였으며, 에리소르빌 미리스테이트의 반수 최대 유효농도(EC_{50})는 ABTS assay에서는 34.43±1.54 μM 그리고 DPPH assay에서는 35.77±0.04 μM으로 나타났다. 마지막으로 에리소르빌 미리스테이트의 항균능의 경우, *Staphylococcus aureus* (최소저해농도: 0.50-0.60 mM, 최소사멸농도: 0.60-1.00 mM)와 *Bacillus cereus* (최소저해농도: 0.025-0.10 mM, 최소사멸농도: 0.05-0.10 mM)와 같은 그람 양성균 식중독균에 대해 정균 효과 및 사멸 효과가 나타났지만, *Escherichia coli*와 S*almonella* Typhimurium와 같은 그람 음성 식중독균에서는 효과가 나타나지 않았다. 투과전자현미경 분석은 에리소르빌 미리스테이트의 항균능 기작이 균의 세포막의 투과성을 변화시키는 원리에 기반하였음을 제시하였다. 결론적으로 본 연구에서 개발한 에리소르빌 미리스테이트은 항산화능과 항균능을 가지는 다기능성 식품 유화제로서 사용되어, 유화 식품의 품질 및 안전성 향상에 도움을 줄 것으로 기대된다.

주제어: 에리소르빌 미리스테이트, 라이페이스-촉매 에스터화 반

응, 다기능성 유화제, 유화능, 항산화능, 항균능

학번: 2018-23305